JOURNAL OF CATALYSIS 81, 450–463 (1983)

On the Activity of Fischer–Tropsch and Methanation Catalysts: A Study Utilizing Isotopic Transients

P. BILOEN,[1] J. N. HELLE, F. G. A. VAN DEN BERG, AND W. M. H. SACHTLER

Koninklijke/Shell-Laboratorium Amsterdam (Shell Research B.V.), Badhuisweg 3, Amsterdam, The Netherlands

Received July 20, 1982; revised December 22, 1982

Stepwise switches from a $^{12}CO/H_2$ to a $^{13}CO/H_2$ feed and vice versa have been utilized to obtain transient kinetic information without disturbing the steady-state catalysis. In the context of methanation and Fischer–Tropsch catalysis it emerges that of the large carbidic overlayer which develops only a small part belongs to reaction intermediates proper. Under the prevailing conditions the fractional coverage in growing chains is low and, consequently, the chain growth relatively fast, i.e., not rate-determining. Details in the relaxation behavior are suggestive of intermediates that are carbidic in nature.

INTRODUCTION

For a rational comparison of the activities of different catalysts it is useful to use turn-over numbers[2] (TONs), defined as reaction rates per surface-exposed atom. Whenever possible it would be very informative to go one step further and dissect the overall TON into two factors:

$$\text{TON} = \theta_s \cdot \text{iTON} \qquad (1)$$

in which

$$\theta_s = \frac{\text{(number of active sites)}}{\text{(number of surface-exposed atoms)}}$$

the so-called Taylor fraction (*1*), and

iTON = the reaction rate per active site.

According to this equation, the overall activity would be determined by two different factors, viz. (a) the density of the active sites (θ_s) and (b) the intrinsic activity of these sites (iTON). Thus, it would be interesting to investigate the effects of, for instance, catalyst preparation methods, addition of promoters, and changes in reaction conditions on θ_s and iTON separately. Note that Eq. (1) assumes uniform activity (i.e., one value for iTON, and therefore for θ_s), which is an approximation. The quantities θ_s and iTON are thus essentially model parameters, and related to this is the lack of straightforward procedures to measure them.

Procedures for arriving at estimates of the parameters θ_s and iTON in Eq. (1) involve (a) absolute-rate-theory-based interpretations of experimentally determined pre-exponentials (*2*), (b) selective poisoning experiments (*3*), and (c) model-based interpretations of transient kinetic experiments (*4, 5*). It is on a particular version of transient kinetics, applied in the context of Fischer–Tropsch and methanation catalysis, that we wish to report here.

In methanation and Fischer–Tropsch catalysis CO is hydrogenated to methane and higher hydrocarbons over transition-metal catalysts such as Ni, Fe, Ru, and Co. Compared to other transition-metal-catalyzed hydrogenations, such as that of olefins to paraffins, the attainable TONs are modest only, i.e., typically of the order of 10^{-2}–10^{-1} mole CO converted/surface-exposed transition metal atom/second (*6*). Two recent studies (*7, 8*) have addressed the question of what limits the activity of Fischer–

[1] Present address: 1240 Benedum Hall, University of Pittsburgh, Pittsburgh, Pennsylvania 15261.

[2] The term turn-over number is being used for what, according to a dimensional analysis, should be called turn-over frequency.

0021-9517/83 $3.00

Tropsch catalysts, both using transient kinetics. Utilizing different catalysts and different methods the respective authors arrived at contrary conclusions with regard to the order of magnitude of the density of active sites, viz. $\theta_s \approx 1$ (*7*) versus $\theta_s \ll 1$ (*8*). We reasoned that the rather drastic methods used in these two studies for generating the transient could have caused side effects, such as the occurrence of irreversible changes in either the adlayer (*7*) or in the catalyst itself (*8*). We therefore concentrated on a method for generating the transient that leaves both the adlayer and the catalyst essentially unperturbed.

In the present work we generate the transients by changing abruptly the isotopic composition of the feed from $^{12}CO/H_2$ to $^{13}CO/H_2$ or vice versa. As we keep the ($^{12}CO + {}^{13}CO$) partial pressure constant the steady-state catalysis proceeds essentially unperturbed, as testified by on-line GLC. The isotopic composition of the product, however, has to adapt itself to the isotopic composition of the feed. The perturbation being an abrupt switch from $^{12}CO/H_2$ to $^{13}CO/H_2$, the transient phenomenon in this experiment is the relaxation of the product from the old composition ($^{12}C_xH_y$) to the new one ($^{13}C_xH_y$). We measured this response by on-line mass spectrometry (Fig. 1), and obtained response (relaxation) curves such as those shown in Fig. 2.

Happel (*9*), who previously called attention to the virtues of this method, applied it to, among other reactions, the methanation over nickel (*10*). In the Discussion we will draw upon his method of interpreting the data, and compare our methanation results with his. We will show that under certain restrictions the response time τ, the coverage in surface intermediates θ_i, and the TON are related as follows:

$$\text{TON} = \theta_i \cdot \tau^{-1} \qquad (2)$$

This formula bears a close resemblance to Eq. (1). The important difference is that Eq. (2) relates TON to the coverage in surface intermediates (θ_i), whereas Eq. (1) relates TON to the coverage in active sites (θ_s).

The present study provides data on the coverage in active intermediates in the production of methane and higher hydrocarbons (Fischer–Tropsch synthesis) over nickel, cobalt, and ruthenium catalysts. It emerges that these data allow conclusions to be drawn regarding both the extent of participation of the carbidic overlayer and the rate of chain growth in the Fischer–Tropsch reaction. Moreover, it emerges

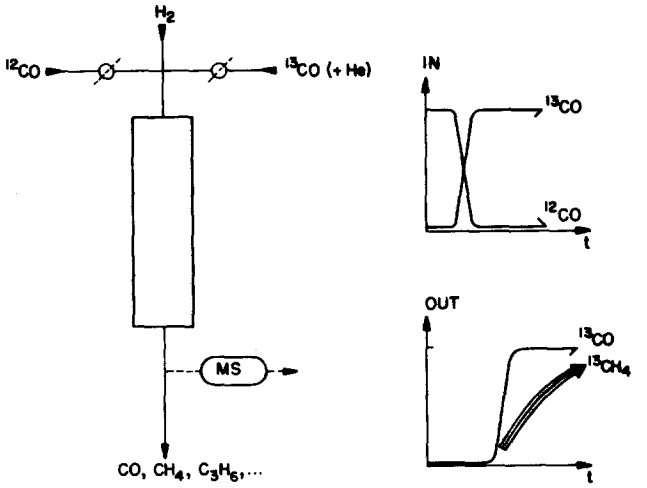

FIG. 1. Experimental configuration with input and output signals.

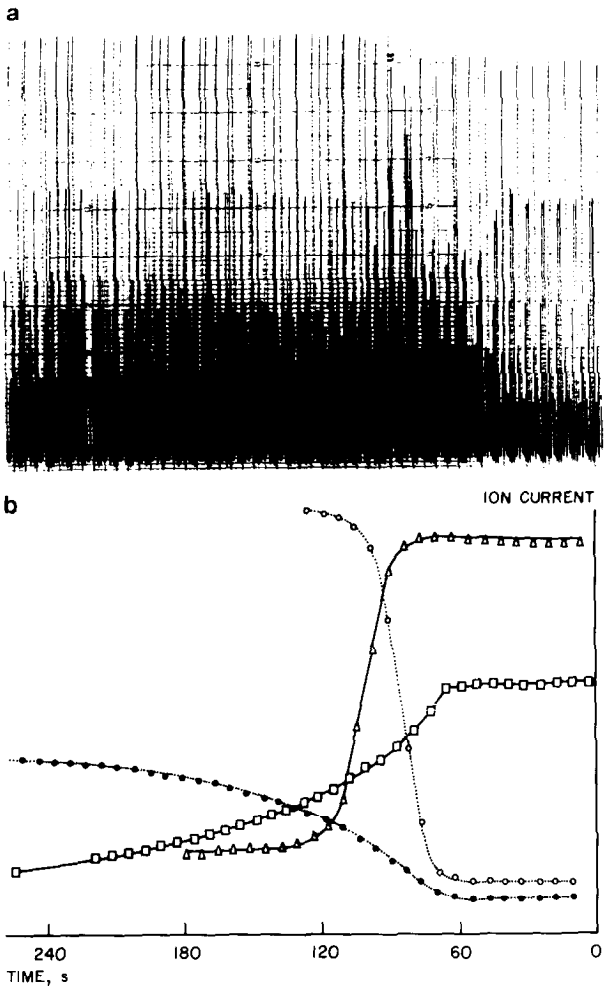

FIG. 2. Primary data (a: repetitive mass spectrometer scans in the mass region 14–30) lead to isotopic transients (b: △, e/m = 29, ^{13}CO; ○, e/m = 28, ^{12}CO; □, e/m = 17$\begin{cases} ^{13}CH_4 \text{ ex } ^{13}CH_4; \\ OH \text{ ex } H_2O \end{cases}$ ●, e/m = 15, $^{12}CH_3$ ex $^{12}CH_4$).

that, unexpectedly, the relaxation data furnish mechanistic information.

EXPERIMENTAL

Catalysts. (1) Unsupported cobalt was prepared according to Ref. (*11*), i.e., via precipitation of cobalt(II) nitrate with concentrated ammonium hydroxide, followed by calcination and temperature-programmed reduction in flowing hydrogen (10 liters H_2/g Co_3O_4/h, ΔT = 4°C/min up to 250°C; 5 h reduction at 250°C). According to XRD the finished catalyst consisted of hexagonal α-cobalt exclusively. It had a BET surface area of 10 m^2/g and a bulk density of 3.0 g/ml.

(2) Ni/SiO_2 (60%w) (Harshaw, 104T) was reduced in flowing hydrogen for 2 h at 480°C. The nickel surface area, according to Ref. (*10*), was approximately 22 m^2/g. The catalyst bulk density was 1.1 g/ml. The catalyst was ground and sieved to mesh size 140-70, and diluted with SiC in a ratio of 1 : 3.

(3) $Ru/\gamma\text{-}Al_2O_3$ (3%w) was prepared by dry impregnation with $RuCl_3$. Reduction was carried out in flowing hydrogen at 400°C for 2 h. The finished catalyst had a

ruthenium surface area of 7.5 m^2/g, as measured by oxygen chemisorption, and a bulk density of 0.6 g/ml.

Equipment and procedure. The experiments were carried out in a plug-flow reactor, with a gas phase hold-up between feed inlet and mass spectrometer of approximately 50 ml, and a catalyst bed of approximately 4 ml. Gas phase hold-up times were calculated from calibration experiments with block pulses of helium. The helium response as monitored at the reactor outlet rose in approximately 14 s from the 20% to the 80% level, and the symmetrical shape of the response curve (Fig. 3) indicated back-mixing effects to be essentially absent.

Isotope analyses were performed with a quadrupole mass analyser, connected to the reactor outlet via a low-pressure ($P \approx 10^{-3}$ bar) line (i.e., pumped capillary), which effectively eliminated any hold-up and back-mixing effects. The relaxation curves were determined by repetitive scans with the mass spectrometer, each scan encompassing either the mass regions 14–17 (CH_4) plus 28–24 (CO) (repetition interval 7 s) or the mass region 39–47 (C_3H_6) (repetition interval 24 s). The latter mass region also contained minor contributions from higher hydrocarbons.

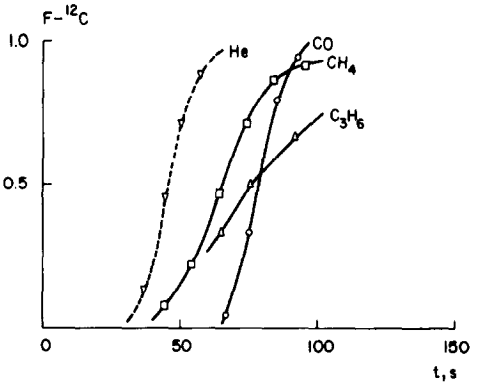

FIG. 3. Relaxation curve: Ru-2. Time-on-stream: 4.0 h. TON^{-1}–CH_4 = 200 s/(mol/surf. exp. at.). TON^{-1}–C_3 = 667 s/(mol/surf. exp. at.).

RESULTS

Catalytic activities were determined with on-line GLC, calibrated in order to obtain absolute rates of production of CH_4 and (C_3H_6 + C_3H_8). A steady-state level of activity was usually attained within 30 min. Thereafter the activity decreased slowly. Table 1 lists the activities (TONs) together with the pertaining process conditions.

TABLE 1

Activities (Quoted as TONs, i.e., Moles Product/Surface-Exposed Atom/*s*)

Cat.-exp.	Time-on-stream (h)	TON (CH_4)	TON (C_3H_6 + C_3H_8)[a]
Ni-1	0.5	8×10^{-4}	8×10^{-5}
Ni-2	21.0	5×10^{-4}	3.5×10^{-5}
Ni-3	21.2	5×10^{-4}	3.5×10^{-5}
Co-1	0.25	6.6×10^{-3}	9.7×10^{-4}
Co-2	5.8	4.9×10^{-3}	6.5×10^{-4}
Co-3	6.0	4.9×10^{-3}	6.5×10^{-4}
Ru-1	0.5	6.6×10^{-3}	2.1×10^{-3}
Ru-2	4.0	5.0×10^{-3}	1.5×10^{-3}

Conditions	CO/H_2 (v/v)	Total pressure (bar)	GHSV ($l.^{-1}$ h^{-1})	Temperature (°C)
Ni	1/3	3	4000	215
Co	1/5	3	3000	215
Ru	1/5.6	3	2650	210

[a] Selectivity: molar ratio $C_3H_6/C_3H_8 \geq 1$.

The TONs, quoted in Table 1 as moles produced per surface-exposed transition metal atom per second, were obtained with the help of surface-area data pertaining to fresh catalysts. Comparative XRD data from fresh and spent catalysts did not indicate the occurrence of substantial sintering or redispersion during the catalytic runs. The TONs were generally in line which what could be expected on the basis of other kinetic studies (*6, 7, 11*).

Figures 3 to 8 give representative examples of the relaxation curves obtained using on-line mass spectrometry. These curves have been plotted as fractional isotopic compositions versus time. For a $^{12}CO/H_2 \rightarrow {}^{13}CO/H_2$ switch we give ^{13}CO/total CO, $^{13}CH_4$/total CH_4, and $^{13}C_3H_8$/total C_3H_8, with the numerator changed from 13 to 12 for the reverse switch $^{13}CO/H_2 \rightarrow {}^{12}CO/H_2$. Horizontally we plot the time (seconds) elapsed after switching from $^{12}CO/H_2$ to $^{13}CO/H_2$ or vice versa. The dashed helium breakthrough curves are derived from separate calibration experiments, except in the case of Ru-2 (Fig. 3), where helium was present as an internal standard. The delay between helium and CO breakthrough, interpreted as a chromatographic effect (*4*), is discussed further below.

Above a Fischer–Tropsch chain growth probability $\alpha = 0.5$ we observe abrupt changes in the shape of the relaxation curves, which we attributed to distortion by diffusion through a product adlayer. The prevailing data have therefore been collected at $\alpha \leq 0.5$, using the H_2/CO ratio for adjusting the chain growth probability. The constraint in α value resulted in a sensitivity limitation for the detection of higher hydrocarbons. Quantitative data are confined to propene.

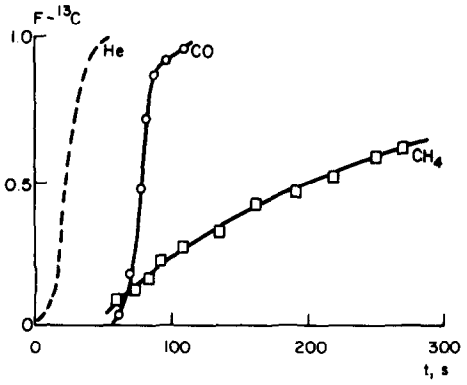

FIG. 5. Relaxation curve: Ni-2. Time-on-stream: 21.0 h. TON^{-1}–CH_4 = 2000 s/(mol/surf. exp. at.). TON^{-1}–C_3 = 28,500 s/(mol/surf. exp. at.).

DISCUSSION

Aspects underlying the interpretation are discussed in Section 1; a manageable procedure for assessing the upper limits for coverages in reactive intermediates is being de-

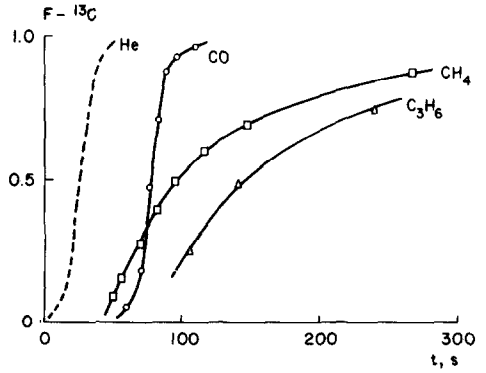

FIG. 4. Relaxation curve: Ni-1. Time-on-stream: 0.5 h. TON^{-1}–CH_4 = 1250 s/(mol/surf. exp. at.). TON^{-1}–C_3 = 12500 s/(mol/surf. exp. at.).

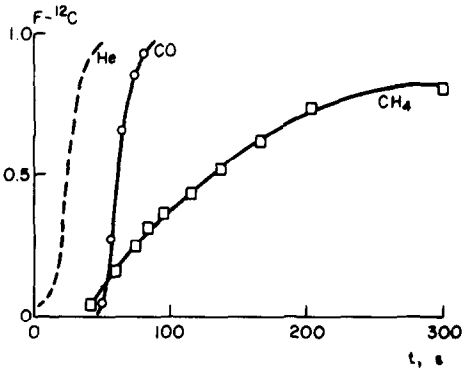

FIG. 6. Relaxation curve: Ni-3. Time-on-stream: 21.2 h. TON^{-1}–CH_4 = 2000 s/(mol/surf. exp. at.). TON^{-1}–C_3 = 28,500 s/(mol/surf. exp. at.).

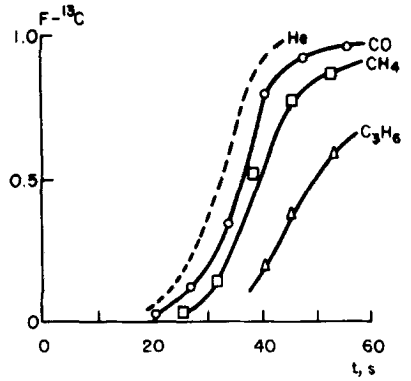

FIG. 7. Relaxation curve: Co-2. Time-on-stream: 5.8 h. TON^{-1}–CH_4 = 202 s/(mol/surf. exp. at.). TON^{-1}–C_3 = 1547 s/(mol/surf. exp. at.).

vised. In Section 2 this procedure is applied to our prevailing data.

1. *Interpretation of Relaxation Data*

1a. Surface-intermediate concentrations in the single-CSTR approximation. We have followed and expanded upon the treatment by Happel *et al.* (*9, 10*), in which the relaxation response emerges as the surface analog of the response of a continuous stirred-tank reactor (CSTR). In this section we confine ourselves to the case of a homogeneous catalyst surface, covered with only a single type of reaction intermediate.

Let us consider (Fig. 9) an arbitrary area of the catalyst surface, containing N_s surface-exposed catalyst atoms. At steady state this surface is covered with a pool of N_i surface intermediates, and produces R product molecules per second. One particular kind of molecule in the feed contains atoms of element E which, at $t = t_0$, are replaced abruptly by an isotopic variant E^1. A simplifying but nonessential assumption is that $E(E^1)$ is present in only one kind of reactant molecule, and that all these reactant molecules, as well as the surface intermediates and product molecules, contain only one atom $E(E^1)$. Further nontrivial restrictions are the following:

(a) There is no hold-up besides the one to be considered explicitly. A switch from E to E^1 in the feed at $t = t_0$ therefore implies that each molecule entering the pool at $t \geq t_0$ contains E^1 instead of E, and that there is no time delay between its leaving the pool and appearing as a product molecule in the gas phase at the reactor outlet.

(b) The surface reaction is unidirectional, i.e., atoms of the marker element $E(E^1)$ enter on the left-hand and leave *only* on the right-hand side (cf. Fig. 9 with Fig. 11).

(c) The rate of mixing in the pool is fast compared with the rate of change in its iso-

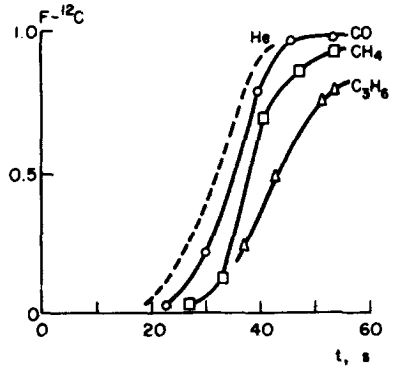

FIG. 8. Relaxation curve: Co-3. Time-on-stream: 6.0 h. TON^{-1}–CH_4 = 202 s/(mol/surf. exp. at.). TON^{-1}–C_3 = 1547 s/(mol/surf. exp. at.).

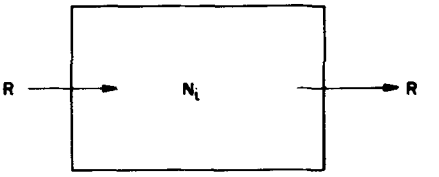

SINGLE POOL RESPONSE:

$$F = 1 - e^{-t/\tau}$$

WITH:

$$\tau = \frac{N_i}{R} = \frac{N_i/N_s}{R/N_s} = \frac{\theta_i}{TON}$$

FIG. 9. Single pool response.

topic composition (CSTR approximation).

Designating the isotopic composition of the pool by

$$F(t) = \frac{N_{E^1}}{N_E + N_{E^1}} = \frac{N_{E^1}}{N_i} \quad (3)$$

we have at $t > t_0$

$$\left(\frac{dN_{E^1}}{dt}\right)_{in} = R \quad (4)$$

and

$$\left(\frac{dN_{E^1}}{dt}\right)_{out} = R \cdot F(t), \quad (5)$$

Therefore

$$\frac{dN_{E^1}}{dt} = \left(\frac{dN_{E^1}}{dt}\right)_{in} - \left(\frac{dN_{E^1}}{dt}\right)_{out} = R \cdot [1 - F(t)] \quad (5a)$$

with $dN_{E^1} = N_i dF$ (cf. Eq. (3)) and $dF = -d(1 - F)$. This leads to

$$- N_i \cdot \frac{d[1 - F(t)]}{dt} = R \cdot [1 - F(t)] \quad (6)$$

which upon integration yields

$$F(t) = 1 - e^{-(t-t_0)/\tau} \quad (7)$$

with

$$\tau = \frac{N_i}{R}. \quad (8)$$

The sequence (3)–(8) is characteristic of any CSTR problem. However, a result characteristic of a surface reaction originates when we divide both the numerator and the denominator of Eq. (8) by N_s, the number of surface-exposed catalyst atoms:

$$\tau = \frac{N_i/N_s}{R/N_s} = \frac{\theta_i}{\text{TON}}, \quad (9)$$

in which θ_i is the fractional coverage in surface intermediates.

Equation (9) can be rewritten as

$$\text{TON} = \theta_i \cdot \tau^{-1} \quad (10) = (2)$$

which has the same form as Eq. (1), albeit with different quantities on the right-hand side.

Under restriction (a) the isotopic composition of the pool, $F(t)$, is identical to what is measured at the reactor outlet by the mass spectrometer. It follows that under constraints (a)–(c) the relaxation curve monitored by mass spectrometer is a purely exponential one (cf. Eq. (7)), i.e., a curve fully characterized by one parameter, viz. the relaxation time τ. According to Eq. (9) we are able to calculate from τ the coverage in surface intermediates, θ_i, provided that we have, from independent measurements, a value for the reaction rate per surface-exposed atom (TON).

1b. A method for dealing with series of reaction steps. The single-CSTR (pool) approximation of the preceding paragraph represents the case of a catalyst surface covered with only one type of surface intermediate. It supposes a sequence

$$A(g) \rightarrow X_{ads} \rightarrow B(g)$$

whereas a substantial fraction of surface reactions involves more than one (kinetically significant) surface intermediate, with a simple sequence:

$$A(g) \rightarrow X_{ads} \rightarrow Y_{ads} \rightarrow B(g)$$

already corresponding to two pools of surface intermediates, X_{ads} and Y_{ads}, connected as CSTRs in series. With $\mathbb{N}$ pools one expects response curves characterized by $\mathbb{N}$ (relaxation) constants instead of one. It therefore is not surprising that the curves actually measured (Figs. 3–8) deviated from the purely exponential one, characterized by a single relaxation time (Eq. (7)). Thanks to the linear nature of $F(t)$-determining equations such as Eq. (6) (R independent of $F(t)$) it is possible to obtain analytical solutions for complex cases. Specific examples have been given by Happel *et al.*, who have also discussed the problem relating to ambiguity in the choice of an appropriate model (*9, 10*).

In order to deal with some of the unknown aspects of the reaction sequence, confining ourselves to a sequence of an un-

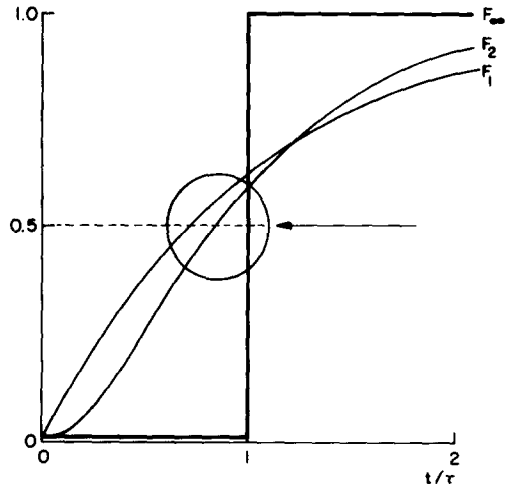

FIG. 10. Effect of dividing a pool of fixed size into subpools: $t(F = 0.5)$ increases.

known number, $\mathbb{N}$, of elementary reaction steps in series, we propose the following procedure. We consider a *fixed coverage*, θ_i, in surface intermediates, divided into an unknown number, $\mathbb{N}$, of different pools. The analog is a CSTR of *fixed volume*, staged into $\mathbb{N}$ compartments. What is being considered then is the effect of staging on the hold-up time. For reasons of simplicity, although this is not essential for the conclusions to be reached, we take the $\mathbb{N}$ compartments to be of equal volume. With the boundary condition that the "total CSTR volume is constant" the response is a function of two variables only, viz. $\mathbb{N}$ and V_{total}/R. For the two limiting cases $\mathbb{N} = 1$ and $\mathbb{N} = \infty$ (ideal plug flow) the response is shown in Fig. 10. Analytical solutions for general $\mathbb{N}$ are available (*12*), and from inspection of (*13*) and Fig. 10 it emerges that

$$F_{\mathbb{N}}(t) \leq F_1(t) \text{ for } F_1 \leq 0.5.$$

This result is equivalent to the statement that staging delays the initial phase of the mixing in a CSTR, and is not confined to stages of an equal volume. We therefore conclude that the effect of the presence of several instead of one pool of intermediates (or series of reaction steps) amounts to an *increase* of $t_{\frac{1}{2}}$ beyond the value given by the same number of surface species present in *one* pool.

Our present method of data analysis is based on the foregoing. We treat our data as if they were generated by *one* pool: $F = 1\text{-exp}[-t/\tau]$ and $t(F = 0.5) = \tau/\ln 2$. From our relaxation curves we determine $t_{\frac{1}{2}}$ and calculate

$$\tau^* \equiv \frac{t_{\frac{1}{2}}}{\ln 2} \qquad (11a)$$

We substitute the τ^* value so obtained into Eq. (10), the response for a single homogeneous pool, and obtain

$$\theta_i^* \equiv \frac{\tau^*}{\text{TON}^{-1}} \quad \text{(cf. Eq. (10))}. \qquad (11b)$$

According to the foregoing θ_i^* is an *upper limit* for the total coverage, θ_i, in surface intermediates.

For a product molecule containing several atoms of the marker element carbon the $t_{\frac{1}{2}}$ value should refer to that particular moment in time at which the *atomic* content of the product in the "new" marker has risen to 50%. With our data output being too slow to follow the rise and fall of intermediates such as $^{13}C_1{}^{12}C_2H_8$ and $^{13}C_2{}^{12}C_1H_8$ we used an adopted definition (cf. Results) in which $t_{\frac{1}{2}}$ (Table 2) refers to that instant at which 50% of the product stream consists of *molecules* entirely built from marker atoms of the new type (i.e., $^{13}C_3H_8$ for a switch $^{12}CO/H_2$ $^{13}CO/H_2$). One easily verifies that this procedure reinforces the nature of θ_i^* as being an upper limit.

Surface heterogeneity transforms Eq. (8) into a more complicated one:

$$\text{TON} = \sum_k \theta_{i,k}\tau_k^{-1} \qquad (8a)$$

As the model analog is closer to that of CSTRs connected in parallel than to that of serial connection, the effects of surface heterogeneity are *not* covered by the above procedure.

1c. Reversible instead of unidirectional steps. In the derivation of Eq. (8) we had to confine ourselves to unidirectional reac-

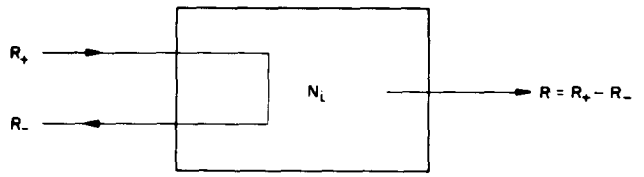

$$\tau = \frac{N_i}{R_+}$$

$$= \frac{N_i}{R\left(1 + \frac{R_-}{R}\right)}$$

C.f. $\tau = \frac{N_i}{R}$ FOR UNIDIRECTIONAL STEP ($R_- = 0$)

FIG. 11. Bidirectional step.

tions (cf. Section 1a). We reconsider the derivation of Eq. (8) for the reversible step (Fig. 11).

$$A(g) \rightleftharpoons P_{ad} \rightarrow Q_{ad} \rightarrow B(g).$$

We have (Fig. 11)

$$\left(\frac{dN_{E^1}}{dt}\right)_{in} = R_+ \qquad \text{(cf. Eq. (4))}$$

and

$$\left(\frac{dN_{E^1}}{dt}\right)_{out} = (R_- + R) \cdot F(t) = R_+ \cdot F(t)$$

(cf. Eq. (5))

and therefore

$$\tau = \frac{N_i}{R_+} \qquad \text{(cf. Eq. (8))} \qquad (12)$$

which is equivalent to

$$\theta_i = \left(\frac{\tau}{\text{TON}^{-1}}\right)\left(1 + \frac{R_-}{R}\right)$$

(cf. Eq. (9)). (13)

It follows that for pools such as P_{ad} we may underestimate the size by using eq. (9) instead of (13). The size of such pools, further designated as *not* being separated from the feed ($A(g)$) by at least one unidirectional step, is therefore not subject to the upper-limit estimation obtained from Eq. (11b). In the prevailing context of methanation and Fischer–Tropsch synthesis CO_{ad} constitutes such a pool.

It is worth noting that the pool P_{ad} is a delaying element in the overall sequence of steps (positive contribution to $t_{\frac{1}{2}}$). Its very presence therefore reinforces the nature of θ_i^* (Eq. (11b)) as being an upper limit for the total coverage in intermediates which *are* separated from the feed by at least one unidirectional step.

1d. Chromatographic effects. In Figs. 3 and 7–8 we have taken the instant of switching isotopes at the reactore *inlet* as $t = 0$. As we monitor the relaxation curves at

TABLE 2

$t_{1/2}$ Values[a] from Relaxation Experiments

Cat.-exp.	$t_{1/2}$[b]–CO (s)	$t_{1/2}$[b]–CH_4 (s)	$t_{1/2}$[c]–C_3H_6 (s)
Ni-1	52	71	122
Ni-2	53	186	—
Ni-3	36	106	—
Co-2	4	7	17
Co-3	3	6	11
Ru-1	19	14	—
Ru-2	32	19	30

[a] Corrected for hold-up in the gas phase, i.e., $t = 0$ at breakthrough of helium at the reactor outlet.

[b] Defined as t(% ^{13}C in product equals 50).

[c] Defined as t(% $^{13}C_3H_6$ in total C_3H_6 equals 50) for $^{12}CO/H_2 \rightarrow {}^{13}CO/H_2$.

TABLE 3

Steady-State Coverage in CO of Working Catalysts, Calculated from CO Retention (Chromatographic Effect)

Parameter	Catalysts		
	Ni/SiO_2	Co-precip.	$Ru/\gamma\text{-}Al_2O_3$
CO retention time, relative to He (s)	52	4	32
Adsorbed CO (ml g^{-1})[a]	13	.19	5.9
Adsorbed CO (ml g^{-1})[b]	8.2	3.7	2.8
(CO/metal) as determined from the chromatographic effect.	1.6	0.05	2.1

[a] Calculated as retention time (s) × CO flow (ml g^{-1} s^{-1})
[b] Calculated from independent dispersion data, when assuming (CO/metal) = 1.

the reactor *outlet* we have corrected the monitored values of $t_{\frac{1}{2}}$ for hold-up in the gas phase (Table 2). In experiment Ru-2, for example, we included a small amount of He in the "new" CO. The helium appears after approximately 46 s at the reactor outlet (Fig. 3), consistent with a gas phase volume between reactor inlet and the mass spectrometer of some 46 ml and a flow rate of about 1 ml/s at 3 bar. We observe $F = 0.5$ for CH_4 and C_3H_8 at $t = 65$ s and $t = 76$ s, respectively (Fig. 3), represented in Table 2 as 19 and 30 s, respectively.

Whereas the relaxation curves for CH_4 and C_3H_8 conform roughly to Eq. (7) with $t_0 = 46$ s, the breakthrough curve for the "new" CO behaves in an entirely differently way. It runs parallel to the helium curve, corresponding to $\tau \approx 0$, i.e., fast equilibration CO(g) $\rightleftharpoons$ CO(ads). However, it lags behind the helium curve by approximately 30 s. We ascribe this to a chromatographic effect (*4*) analogous to what happens in frontal analysis chromatography: it takes a finite retention time (approximately 30 s) to displace "old CO-ads" by "new CO-ads."

In Table 3 we have listed values for CO/Me, calculated by combining CO-retention data with dispersion data. Whereas one expects to find CO/Me values close to 1.0 (*14*) we find CO/Ni = 1.6 and CO/Ru = 2.1. In view of the accumulated uncertainties we consider the agreement to be satisfactory. The overall picture is consistent with high CO coverage and fast CO exchange, as concluded earlier (*15*). The value CO/Co = 0.05, however, is surprisingly low. Additional independent dispersion measurements (XRD line broadening, SEM, and hydrogen chemisorption) all yielded values between 10 and 20 m^2/g, i.e., of the same order of magnitude as found in the BET measurement. We have no unambiguous explanation for the low steady-state CO/Co value emerging from the (small) chromatographic effect.

Retention increases $t_{\frac{1}{2}}$ and therefore also reinforces the upper-limit nature of θ_i^*. For the limiting case $\theta_i = 0$ (i.e., $\tau = 0$) we indicated schematically in Fig. 12 the effect of CO retention on the product relaxation curve. A comparison of Fig. 12 with Fig. 3 actually indicates a substantial part of the $\Delta t_{\frac{1}{2}}$–CH_4, C_3H_8 (relative to helium) to be CO retention.

2. *Analysis of Results*

2a. Methanation. The relaxation curves for methane (Figs. 3–8) have been treated according to the procedure outlined in Section 1b: $t_{\frac{1}{2}}$ values (Table 2) have been converted into θ_i^* values via Eq. (11a,b). The resulting θ_i^* values vary between 0.04 and 0.14 (Table 4). According to the discussion

TABLE 4

Coverages in Reactive Intermediates Calculated According to $\theta^* = \tau^*/(TON^{-1}) = \Delta t_{\frac{1}{2}}/\ln 2/(TON^{-1})$[a]

Cat.-exp.	Time-on-stream (h)	θ^*–CH_4	θ^*–C_3H_6
Ni-1	0.5	0.08	0.014
Ni-2	21.0	0.13	—
Ni-3	21.2	0.08	—
Co-2	5.8	0.05	0.016
Co-3	6.0	0.04	0.010
Ru-1	0.5	0.13	
Ru-2	4.0	0.14	0.06

[a] TON^{-1} and $\Delta t_{\frac{1}{2}}$ taken from Tables 1 and 2, respectively, with $\Delta t_{\frac{1}{2}}$ relative to *helium*.

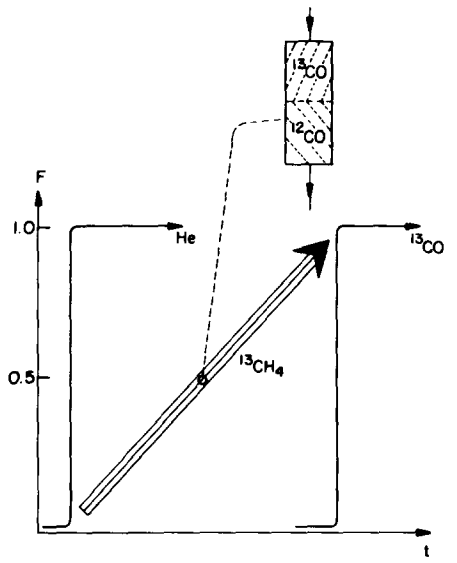

FIG. 12. Retention of CO due to exchange between CO_g and CO_{ad} produces delay between the He and CO breakthrough curves, and introduces an additional inclination in the relaxation curves. The example is given for $\tau_{CH_4} = 0$.

in Sections 1b and 1c these values represent upper limits for the total coverage in those reaction intermediates which are separated from the feed by at least one unidirectional step.

With regard to unidirectionality we mention that at prevailing low temperature and low conversion the overall methanation reaction is strictly unidirectional: $R_+/R_- > 10^6$. It is therefore plausible that in the sequence of elementary steps there is at least one which conforms to the unidirectionality requirement posed by Eq. (13) (Section 1c). For the very location of such step(s) within the sequence we must, however, refer to additional evidence (we note in passing that in this respect the Fischer–Tropsch reaction lends itself much better to analysis; cf. Section 2b). Particularly relevant are studies in which catalysts have been precovered with (labeled) surface carbon and then subjected to CO/H_2. It was found (*15, 16*) that the labeled carbon was transferred to product (CH_4) rather than to unconverted feed (CO). This is indicative of a sequence in which oxygen-ex-CO is being removed, either as CO_2 or as H_2O, in an essentially unidirectional step (1):

$$CO/H_2 \underset{(1)}{\rightarrow} CH_x(+\ CO_2,\ H_2O) \underset{(2)}{\rightleftharpoons} CH_4$$

The proposition that carbidic surface species CH_x (x = 0–3) are reaction intermediates in the methanation reaction proper has also been advanced in several other recent studies (*17, 19, 23*). We therefore propose to identify θ_i^*–CH_4 (Table 4) with the upper limit for the coverage in carbidic intermediate CH_x (x = 0–3).

Two recent studies of methanation over nickel yielded an estimate of the coverage in carbidic intermediates which is of the same order of magnitude as what we report here. Goodman *et al.* (*18*) did experiments with nickel crystals and determined overlayer coverages from AES. Happel *et al.* (*10*) were the first to apply transient isotopic labeling, the method used in the present study. Actually, for comparison, we employed a supported nickel catalyst closely similar to the one used by Happel *et al.* It should be noted that the syngas pressure in our work (3 bar) substantially exceeds that used by Goodman *et al.* and Happel *et al.* CO/H_2 ratios, however, are similar.

Whereas there is satisfying agreement with the results of Goodman *et al.* and Happel *et al.* we note that quite a number of studies led to much higher values for the coverage in carbidic species (*17*). These studies share in essence a procedure in which run-in catalysts at elevated temperature are being exposed to hydrogen in the *absence* of CO. Methane and also higher hydrocarbons are produced in such a procedure, and the large amounts of methane are indicative of a reservoir of "reactive" carbon with a size equivalent to 1–6 monolayers. This is also what we find at present, when we expose the catalysts used in the transient studies to pure hydrogen: the amount of methane produced points to "reactive" carbon well in excess of one monolayer amount (in exceptional cases, with

nickel, up to equivalent of 46 monolayers), whereas the isotopic transients point to an amount of intermediates of the order of 0.1 of a monolayer only. It emerges that of the large carbidic "overlayer" which frequently develops only a small part belongs to intermediates proper.

Probably related to the foregoing is the observation that the relaxation times increase with increasing time-on-stream of the catalysts, the phenomenon being most pronounced with nickel (cf. Figs. 4 and 5). Within the single pool formalism (Section 1b, Eq. (11)) this translates into a coverage in reaction intermediates that increases with time-on-stream. However, when we impose two isotope changes shortly after one another ($12 \rightarrow 13 \rightarrow 12$) on an aged catalyst, we observe, surprisingly, two transients exhibiting different values for $t_{\frac{1}{2}}$ (called hereafter "asymmetry"; cf. Figs. 5 and 6). This phenomenon is absent when we conduct the same sequence with a fresh catalyst. Within the single pool formalism this result suggests that as a consequence of the first transient experiment the coverage in surface intermediates, as monitored with the second transient, has dropped suddenly. As the transients do not disrupt the steady-state catalysis (total CO pressure constant, GLC trace stationary) this conclusion is untenable.

With regard to this asymmetry we notice that:

(a) There is an asymmetry in the exposure history of the catalysts as well, specifically after prolonged time-on-stream. This asymmetry originates from the fact that, except for short intervals, the catalyst ages under $^{12}CO/H_2$ rather than under $^{13}CO/H_2$.

(b) A *single* pool responds essentially symmetrically: two subsequent transients should exhibit identical τ values, even when the time interval between the two transients is too short to allow for complete relaxation of the pool ($F = \alpha(1 - e^{-t/\tau})$ instead of $F = (1 - e^{-t/\tau})$ with $\alpha \leq 1$).

We therefore conclude that a proper description of the "asymmetry phenomenon" has to include *two* pools at least.

We propose the configuration depicted in Fig. 13, with two pools positioned in parallel. This configuration leads to an asymmetry as observed in the present case (*13*) when the time interval between two transients is too short to allow for relaxation of pool II: at the start of transient 1, i.e., after several hours of exposure to $^{12}CO/H_2$, the isotopic composition of pool I and II is identical, whereas at the start of transient 2, i.e., after 0.2 h exposure to $^{13}CO/H_2$, their isotopic compositions differ ($F_{13,I} > F_{13,II}$).

We propose to identify reservoir I (Fig. 13) with the carbidic surface intermediates proper, and to identify reservoir II with the remainder of the carbidic "overlayer." To explain our observations we then have to assume that reservoir II develops only after substantial time-on-stream of the catalyst. This is consistent with e.g. the surface studies of Goodman *et al.* (*18*) and of Bonzel and Krebs (*19*), in which it was concluded that during actual catalysis amorphous reactive carbon slowly deteriorates to form less reactive graphitic carbon. That the phenomenon is most pronounced with nickel fits in with previous findings (*20*) that nickel, compared to ruthenium and cobalt, has a pronounced tendency to dissolve carbon and to form carbonaceous filaments.

Finally we note that the classification of what probably is a continuous distribution in reactivity into two discrete pools (Fig. 13) is likely to be an oversimplification. However, the relaxation experiments con-

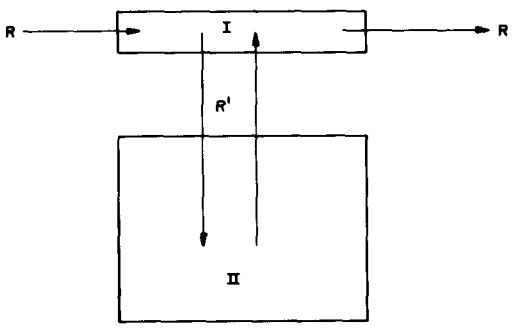

FIG. 13. Pool of surface intermediates (I) communicating with additional reservoir (II).

sistently indicate that of all carbidic species present only a minority fraction effectively participates in methane production. This is one of the main findings in the present relaxation work.

2b. Fischer–Tropsch catalysis. Fischer–Tropsch catalysis seems particularly amenable to analysis by the prevailing method, as the very chain length distribution in product is indicative of "built-in" unidirectionality. The product distribution in Fischer–Tropsch reactions typically obeys Schulz–Flory polymerization statistics:

$$\frac{C_{n+1}}{C_n} = \alpha; \qquad \alpha \leq 1 \tag{14}$$

in which C_n is the molar yield of hydrocarbons with n carbon atoms in their chain, and α is a chain length-independent constant. This indicates that the hydrocarbon chains are being built in a series of independently repeated steps (*21*)

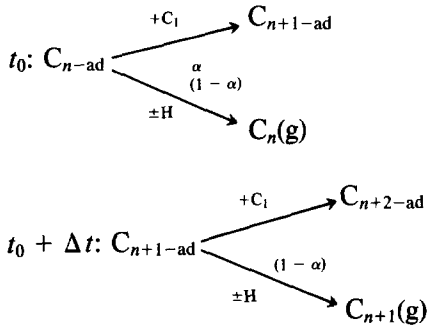

(15)

Significant bidirectionality of the type

$$C_{n-ad} \rightleftharpoons C_{n+1-ad} \tag{16}$$

would lead to replacement of the kinetic control (Eq. (14)) by thermodynamic control (*22*). When C_{n-ad} is used to denote the growing chain (surface intermediate) with n carbon atoms it follows that for $n \geq 2$ C_n is separated from the feed (CO, CO_{ads}) by at least $(n - 1)$ unidirectional steps.

Concentrating on C_3H_6 it follows from the foregoing and the discussion in Section 1b that θ_i^*–C_3H_6 (Table 4) represents an upper limit for the combined coverage in growing chains with two and three carbon atoms. According to Table 4 this coverage amounts to a few percent at most. Moreover, as Eq. (14) also describes the chain length distribution of the ad-species it follows by applying the sum rule for geometric progressions:

$$\sum C_{n+} = \frac{C_n}{1 - \alpha} \tag{17}$$

that the *total* coverage in growing chains is low too (at $\alpha < 0.5$). Therefore, our results fit with recent data of *in situ* ir (*23*), support those of Kieffer (*8*) and do not support those of Dautzenberg *et al.* (*7*) (cf. Introduction), albeit that the differences in catalysts and in reaction conditions hamper a strict comparison.

An analysis equivalent to the foregoing is one in which one considers the quantity Δt of Eq. (15). Owing to the unidirectionality this quantity has a physical meaning, namely, the time interval between two successive chain growth steps. It follows that an upper limit for Δt, Δt^*, is given by:

$$\Delta t^* = (t_{\frac{1}{2}} - C_3H_6)/2. \tag{18}$$

According to Table 2 upper limits for Δt vary from 6 to 60 s, whereas $(TONs)^{-1}$ are between 500 and 10,000 s (Table 1). It therefore emerges that chain growth proper is not rate-determining in Fischer–Tropsch synthesis. This inference which is equivalent to the previous statement that the "coverage in growing chains is low" is another main conclusion from the prevailing work.

Finally, it emerges that after a sufficiently long time-on-stream (under $^{12}CO/H_2$) the cobalt catalyst exhibits asymmetry in the propene relaxation (see Figs. 7 and 8). We refer to Fig. 13 and the accompanying discussion in Section 2a and propose, on the strength of this asymmetry, that the reservoir containing the growing chains, just like the reservoir containing the methane precursors, communicates with reservoir II. According to AES (*18, 19*) reservoir II is carbidic in nature rather than filled

with oxygenates. The observations are suggestive of methane and higher hydrocarbons drawing from a common pool (i.e., reservoir I) of intermediates. This pool probably is that of C_1 intermediates, and as it communicates with the carbidic reservoir II it is probably itself carbidic in nature. In the context of Fischer–Tropsch synthesis the C_1 intermediates are to be identified with the building blocks adding to the growing chain (cf. Eq. (15)). The mechanism of the Fischer–Tropsch reaction has been the subject of a long-standing debate, centering around the question of whether or not the C_1 building blocks contain oxygen (*17*). It emerges that the present, kinetic, experiments give, unexpectedly, independent mechanistic evidence indicating that chain growth in Fischer–Tropsch synthesis involves carbidic CH_x (probably CH_2) building blocks.

ACKNOWLEDGMENTS

The authors gratefully acknowledge the stimulating discussions they had with Dr. J. Happel, Dr. E. P. H. Kieffer, Dr. R. A. van Santen, and Dr. M. C. Valentijn and the capable assistance of Ms. E. Vermont.

REFERENCES

1. Taylor, H. S., *Proc. Roy. Soc. Edinburgh* **A108,** 105 (1925).
2. Maatman, R. W., *Adv. Catal.* **29,** 97 (1980).
3. Turkevich, J., Nozaki, F., and Stamires, D., *Proc. Int. Congr. Catal., 3rd, 1964* **I,** 586, North Holland, Amsterdam, 1965.
4. Furusawa, T., Suzuki, M., and Smith, J. M., *Catal. Rev.* **13,** 43 (1976).
5. Boudart, M., "Kinetics of Chemical Processes," Prentice Hall, Englewood Cliffs, New Jersey, 1968.
6. Vannice, M. A., *J. Catal.* **37,** 462 (1975).
7. Dautzenberg, F. M., Helle, J. N., van Santen, R. A., and Verbeek, H., *J. Catal.* **50,** 8 (1977).
8. Kieffer, E. P. H., Ph.D. Thesis, Technological University, Eindhoven, The Netherlands, 1981.
9. Happel, J., *Chem. Eng. Sci.* **33,** 1567 (1978).
10. Happel, J., Suzuki, J., Kokayeff, P., and Fthenakis, V., *J. Catal.* **65,** 59 (1980).
11. Rautavuoma, A. O. I., Ph.D. Thesis, Technological University, Eindhoven, The Netherlands, 1979.
12. Levenspiel, O., "Chemical Reaction Engineering," 2nd ed., Chapter 9. Wiley, New York.
13. Valentijn, M. C., private communication.
14. Ekerdt, G., and Bell, A. T., *J. Catal.* **58,** 170 (1979).
15. Biloen, P., Helle, J. N., and Sachtler, W. M. H., *J. Catal.* **58,** 95 (1979).
16. Araki, M., and Ponec, V., *J. Catal.* **44,** 439 (1976).
17. Biloen, P., and Sachtler, W. M. H., *Adv. Catal.* **30,** 165 (1981).
18. Goodman, D. W., Kelley, R. D., Madey, T. E., and White, J. M., *J. Catal.* **64,** 479 (1980).
19. Bonzel, H. P., and Krebs, H. J., *Surf. Sci.* **91,** 499 (1980).
20. Lobo, L. S., Trimm, D. L., and Figueiredo, J. L., *Proc. Int. Congr. Catal.*, 5th (Florida 1972), p. 1125. North Holland/American Elsevier, Amsterdam/New York, 1973.
21. Herington, E. F. G., *Chem. Ind. (London)* 347 (1946).
22. van Santen, R. A., private communication.
23. Yamasaki, H., Kobori, Y., Naito, S., Onishi, T., and Tamaru, K., *J. Chem. Soc. Faraday Trans. I* **77,** 2913 (1981).